Received: 12 December 2019 | Accepted: 1 May 2020

DOI: 10.1002/stem.3236

EMBRYONIC STEM CELLS/
INDUCED PLURIPOTENT STEM CELLS

STEM CELLS

Trajectory mapping of human embryonic stem cell cardiogenesis reveals lineage branch points and an ISL1 progenitor-derived cardiac fibroblast lineage

Mimmi M. Mononen[1,2] | Chuen Yan Leung[1] | Jiejia Xu[2] | Kenneth R. Chien[1,2]

[1]Integrated Cardio Metabolic Centre, Department of Medicine, Karolinska Institutet, Huddinge, Sweden

[2]Department of Cell and Molecular Biology, Karolinska Institutet, Solna, Sweden

Correspondence
Kenneth R. Chien, MD, PhD, Department of Cell and Molecular Biology, Karolinska Institute, Biomedicum A6, Solnavägen 9, 17165 Solna, Sweden.
Email: kenneth.chien@ki.se

Funding information
Knut och Alice Wallenbergs Stiftelse, Grant/Award Number: KAW 2013.0028; Croucher Foundation; Swedish Research Council, Grant/Award Numbers: 541-2013-8351, 539-2013-7002; European Research Council Advanced Research Grant Award, Grant/Award Number: AdG743225

Abstract

A family of multipotent heart progenitors plays a central role in the generation of diverse myogenic and nonmyogenic lineages in the heart. Cardiac progenitors in particular play a significant role in lineages involved in disease, and have also emerged to be a strong therapeutic candidate. Based on this premise, we aimed to deeply characterize the progenitor stage of cardiac differentiation at a single-cell resolution. Integrated comparison with an embryonic 5-week human heart transcriptomic dataset validated lineage identities with their late stage in vitro counterparts, highlighting the relevance of an in vitro differentiation for progenitors that are developmentally too early to be accessed in vivo. We utilized trajectory mapping to elucidate progenitor lineage branching points, which are supported by RNA velocity. Nonmyogenic populations, including cardiac fibroblast-like cells and endoderm, were found, and we identified TGFBI as a candidate marker for human cardiac fibroblasts in vivo and in vitro. Both myogenic and nonmyogenic populations express *ISL1*, and its loss redirected myogenic progenitors into a neural-like fate. Our study provides important insights into processes during early heart development.

KEYWORDS

cardiac, differentiation, embryonic stem cells, gene expression, progenitor cells

1 | INTRODUCTION

Cardiogenesis is a complex process involving a family of multipotent cardiac progenitors. Single-cell RNA sequencing (scRNA-seq) studies have revealed temporal and spatial expression patterns of embryonic cardiac populations.[1-5] Compared with murine cardiogenesis, our knowledge on early human progenitor lineages is limited. Two recent studies provided fundamental understandings of the human fetal heart in single-cell resolution.[6,7] However, since the heart is the first organ to develop, the earliest human samples that can be feasibly collected do not cover the onset of cardiogenesis, and therefore, the earliest human progenitor populations have remained elusive. Cardiac induction of human pluripotent stem cells (hPSCs) has emerged as an important model system for early human cardiogenesis and disease modeling.[8-10] Furthermore, a recent study supports the application of hPSC-derived cardiac progenitors as a viable alternative to mature cardiomyocytes in regenerative medicine.[11]

Recent efforts have characterized transcriptional snapshots of the cardiomyocyte and other lineages during hPSC cardiac induction by RNA sequencing.[7,12-16] These studies suggest in vitro cardiac differentiation resembles the early human heart development, and that in vitro

Mimmi M. Mononen and Chuen Yan Leung contributed equally to this work.

[Funding information was added on 14 September 2020 after original online publication].

cardiomyocyte differentiation protocols also generate nonmyogenic cell types.[12,13] However, the transient differentiation dynamics of myogenic and nonmyogenic lineages is not fully described.

Therefore, we focused on the transient cellular identities of early cardiac progenitors through lineage and time. We generated Smart-Seq2 scRNA-seq libraries of cells collected from human embryonic stem cell (hESC) cardiac induction using a widely adopted Wnt-modulation based differentiation protocol.[8,10] We identified cardiac differentiation and nonmyogenic cell types, and verified in vitro cell identities by directly integrating with a human fetal cell dataset published by Cui et al.[1] Trajectory analysis using different methods connected lineage heterogeneity through time, and identified lineage branching points, which we confirmed used RNA velocity, also confirming lineage directionality.[17] From this analysis, TGFBI emerged as a candidate marker for cardiac fibroblasts in vitro and in vivo. Lastly, we investigated the role of ISL1 in both myogenic and nonmyogenic progenitors. Taken together, our study highlights the importance of early progenitor model systems that allows us to study otherwise inaccessible progenitor cells in vivo. Our findings provide a valuable reference for using hESC cardiac induction as a platform for genetic studies and disease modeling.

Significance statement

Despite the large interest in defining the transcriptional profiles of human cardiac cells in single-cell resolution, the transient stages of early human cardiac progenitors have remained elusive. This article defines the differentiation and lineage branching points of human embryonic stem cells into cardiomyocytes, endoderm, and cardiac fibroblast-like cells, and elucidates the role of ISL1 in the development of these cell types. Genetic perturbation studies found that ISL1 may be required to suppress a neural-like cell fate in myogenic progenitors.

2 | MATERIALS AND METHODS

2.1 | Maintenance and cardiac differentiation of hESCs

ES03 hESCs were maintained in Essential 8 Flex Medium (Thermo Fisher Scientific) on Matrigel (Corning, Germany) coated six-well plates and passaged in Versene (Thermo Fisher Scientific). The cardiac differentiation protocol was adapted from Lian et al.[9]

2.2 | Smart-Seq2 library preparation and sequencing

Cells were manually picked using a hand-pulled capillary needle and transferred into Smart-Seq2 lysis buffer with ERCC RNA spike-in mix and snap-frozen. Single-cell libraries were processed into cDNA libraries by following the Smart-Seq2 protocol.[18,19] Library quality control was performed using Bioconductor and Qubit for fragment size and concentration. Barcodes were added using Illumina Nextera XT DNA sample preparation kit with dual indexes. Libraries were pooled into batches and sequencing was performed on Illumina HiSeq 2500 for 50 bp single-end reads.

2.3 | Single-cell RNA sequencing data analysis

Raw sequencing reads were de-multiplexed using bcl2fastq and mapped to the human hg38 genome using TopHat. For quality control, cells with less than 7000 detected genes were excluded. Filtering, normalization, and subsequent analyses were performed as described in the Seurat 3.0 R package tutorial, followed by dimensional reduction and clustering, marker gene identification and cell-cycle scoring. Integration of in vitro and in vivo datasets was performed following the standard workflow for data integration and label transfer in Seurat.

Monocle pseudotime analysis was performed following the online tutorial. The Monocle pseudotime values were imported into the Seurat object and visualized to confirm the correlation between different analysis methods. STRING and PANTHER online analysis tools were used for functional enrichment analyses. Force-directed graphing (FDG) was performed using the igraph R package, and the nearest neighbor matrix was calculated using the method described by Kee et al.[20] RNA velocity calculations were performed according to the Velocyto tutorial. In brief, a .loom file with counts divided in spliced/unspliced/ambigious was produced in Python using the human hg38 genome annotation file and an expressed repeat annotation file from the UCSC genome browser. Subsequent RNA velocity analysis was performed according to Le Manno et al.[17]

2.4 | Immunohistochemistry and immunocytochemistry

Cardiac tissue sections were permeabilized in 0.5% Triton X-100, blocked (3% BSA, 3% normal donkey or goat serum in phosphate-buffered saline [PBS]) and incubated with primary antibodies in blocking buffer overnight. Sections were incubated with secondary antibodies in blocking buffer and counterstained with 4′,6-diamidino-2-phenylindole (DAPI).

Cells grown on cover slips were fixed with 4% paraformaldehyde, permeabilized with 0.5% Triton X-100, and blocked with 3% BSA in PBS. Cells were incubated with primary antibodies in blocking buffer overnight, followed by incubation with secondary antibodies and nuclear counterstaining with DAPI.

Following antibodies were used in this study: HHEX (HPA051894, Atlas Antibodies), ISL1 (39.4D5, DSHB), NKX2-5 (sc-14 033, Santa Cruz), TFAP2A (ab108311, Abcam), TGFBI (ab66957, Abcam), TNNT2 (MS-295-P1, Thermo Fisher Scientific), and vimentin (AB5733, Millipore).

2.5 | Human fetal heart tissue

Human fetal hearts at 6.5 and 10 weeks of gestation were obtained from authorized sources in Karolinska University Hospital with an approved ethical permission (2015/1369-31/2) and appropriate informed consents. The fetal hearts were snap-frozen and cryosectioned at 10 μm thickness for immunostaining.

2.6 | Genetic manipulation of hESCs

Genetic manipulation of ES03 hESCs was performed using the CRISPR/Cas9 system. Briefly, two guide RNAs targeting exon 4 were designed and cloned into PB/CRISPR vector. Three plasmids, pPB-CRISPR-ISL1-g1,-g2 and pCyL43, were transfected into hESCs using B-16 program in Nucleofector 2b device. After 2 weeks of puromycin selection, cells were singularized and seeded to generate single-cell-derived colonies. Single-cell clones were picked, expanded, and genotyped. Loss of *ISL1* expression was verified using standard quantitative PCR (qPCR), immunoblotting, and immunocytochemistry methods. Decreased expression of cardiomyocyte marker TNNT2 was detected by flow cytometry after 14 days of cardiac differentiation.

See supplementary methods for further details for experimental procedures and data analysis.

3 | RESULTS

3.1 | Single-cell RNA sequencing reconstructs a temporal axis and reveals distinct phases of human cardiomyocyte differentiation

To rigorously characterize the transient cellular identities during early human cardiomyocyte differentiation, we used a widely adopted protocol[9] that generates 70% to 90% cardiac troponin (TNNT2) expressing cardiomyocytes from karyotypically normal hESCs (supplemental online Figure 1A,B). Following this protocol, beating cells are first observed around day 8. In order to capture a diverse spectrum of cellular states, we harvested cells spanning from cardiac mesoderm and nonbeating cardiovascular progenitors (days 3-7) to beating cardiac progenitors (days 8 and 9) and phenotypically immature, but functionally competent beating cardiomyocytes (day 15) (Figure 1A). Cells were picked manually from two differentiation batches and in total 1024 Smart-Seq2 single-cell libraries were prepared for scRNA-seq,[18,19] of which 925 cells passed the quality control. RNA spike-ins used in the library preparation confirmed low technical variability between libraries (supplemental online Figure 1C), and the number of genes detected per cell was as expected in both batches (supplemental online Figure 1D).

We proceeded with the Seurat version 3.0 package[21-23] and STRING version 11.0 gene ontology (GO)[24] for downstream analyses. The top variable genes across the dataset were associated with developmental processes, chromatin assembly, and muscle contraction (supplemental online Figure 1E). Principal component analysis of the gene-set (supplemental online Table 1) reconstructed a temporal axis along principal component one (PC1), which was supported by *TNNT2* expression (Figure 1B). Analysis of global transcriptional dynamics across time showed that the batteries of gene expression differ significantly between days 3 and 6 (supplemental online Figure 1F). This suggests that up until day 6 the cells rapidly progress through transient and distinct cellular states, until they reach day 7 where the cellular identity becomes relatively stable.

To partition the cells into distinct populations, unsupervised clustering was performed based on principal components 1-9, and visualized on a *t*-distributed neighbor (t-SNE) projection (Figure 1C,D). Statistically significant (Wilcox test, adjusted *P*-value <.05) positive marker genes were identified for each cluster (supplemental online Table 2) and visualized in a heatmap (Figure 1E). GO analysis and literature review were used to identify biological processes and cell subpopulations (supplemental online Table 3).

Based on marker gene expression (supplemental online Table 2), cluster 0 (C0) consists of pluripotent cells, C1 represents cardiac mesoderm, C2 and C3 represent early cardiac progenitors. C2 and C3 differ in that C3 expresses cell-cycle and proliferative markers. C4 and C5 represent late cardiac progenitors and cardiomyocytes, respectively. C6 potentially consists of proapoptotic myogenic cells, which remained after stringent quality control (see the Methods section). C7 consists of nonmyogenic cells expressing fibroblast and epithelial markers. C8 consists of definitive endoderm-like cells.

Based on the distribution of cell types found in each time point, a myogenic population dominated the differentiation. Pluripotent and mesoderm populations persisted in the differentiation until day 6, when fibroblast-like cells began to emerge and persisted until day 15 and possibly beyond. Endoderm-like cells appeared from day 4 onward and were no longer detected by day 15 (Figure 1F). This is also reflected in the expression of pluripotency, cardiac mesoderm, cardiac transcription factor, and sarcomeric marker genes (Figure 1G). Overall myogenic populations are marked by *CDH2* and nonmyogenic populations are marked by *CDH1* expression (supplemental online Figure 1G). Furthermore, Monocle pseudotime analysis[25-27] of the pluripotent and myogenic cells (clusters 0-5) revealed a continuous cardiomyocyte differentiation axis (supplemental online Figure 1H).

Taken together, different stages of myogenic and nonmyogenic lineage differentiation were reconstructed for further downstream analysis.

3.2 | Direct transcriptional comparison between hESC-derived cardiac cells and the human fetal heart

In vitro-derived cardiac populations have long been associated with in vivo lineages based on selected expression markers and functional parameters. To comprehensively compare the two on a global transcriptomic level, we leveraged a human fetal dataset[1] to compare 5-week fetal heart cells with in vitro-generated cells. We integrated our in vitro dataset with the in vivo (5W) dataset[1] using Seurat 3.0,

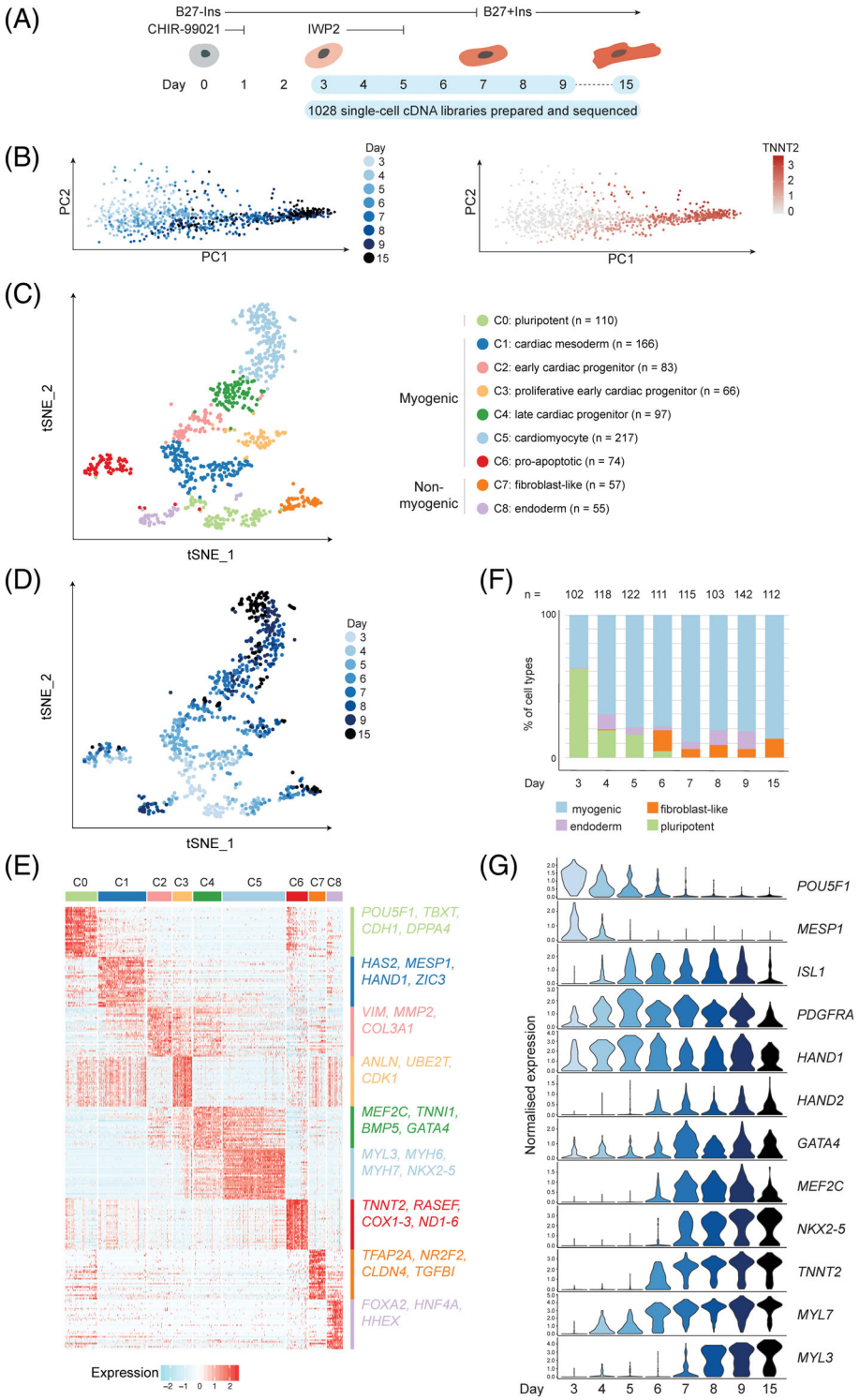

FIGURE 1 Temporal single-cell profiling of human embryonic stem cell (hESC) cardiac induction. A, Schematic representation of hESC cardiac differentiation, with sample collection days indicated in blue. B, PCA plots for 925 cells and 2000 differentially expressed genes. Colors represent time point and *TNNT2* expression. C, D, T-SNE representation of clusters. C, Colors represent clusters. D, Colors represent time point. E, Expression heatmap of the top differentially expressed genes of each cluster. F, Percentage of each cell type per time point: pluripotent (cluster 0), fibroblast-like (cluster 7), endoderm (cluster 8), and myogenic (clusters 1-6). G, Violin plots showing the expression of marker genes of pluripotency and mesoderm development (*POU5F1* and *MESP1*), cardiac transcription factors (*PDGFRA*, *ISL1*, *HAND1*, *HAND2*, *GATA4*, *MEF2C*, and *NKX2-5*), and sarcomeric genes (*TNNT2*, *MYL7*, and *MYL3*) per day

which accounts for different scRNA-seq modalities and parameters such as gene counts per cell[21,23] (see the Methods section) (supplemental online Figure 2A,B). The 5W fetal heart cells did not cluster together with in vitro time points earlier than day 8, but were transcriptionally most similar with in vitro cells across days 8, 9, and 15 (supplemental online Figure 2B). Therefore, we specifically compared 5W cells with day-8, -9, and -15 cells, since there may be a level of asynchronicity across days 8, 9, and 15. To connect the in vivo lineages with their in vitro counterparts, we performed unsupervised clustering on a t-SNE projection (Figure 2A) and GO analysis (supplemental online Figure 2C, Tables 4 and 5). Clustering analysis revealed similar transcriptional profiles between several populations of human fetal and hESC-derived cells, including ventricular cardiomyocytes (integrated cluster 0; IC0), atrial cardiomyocytes (IC1),

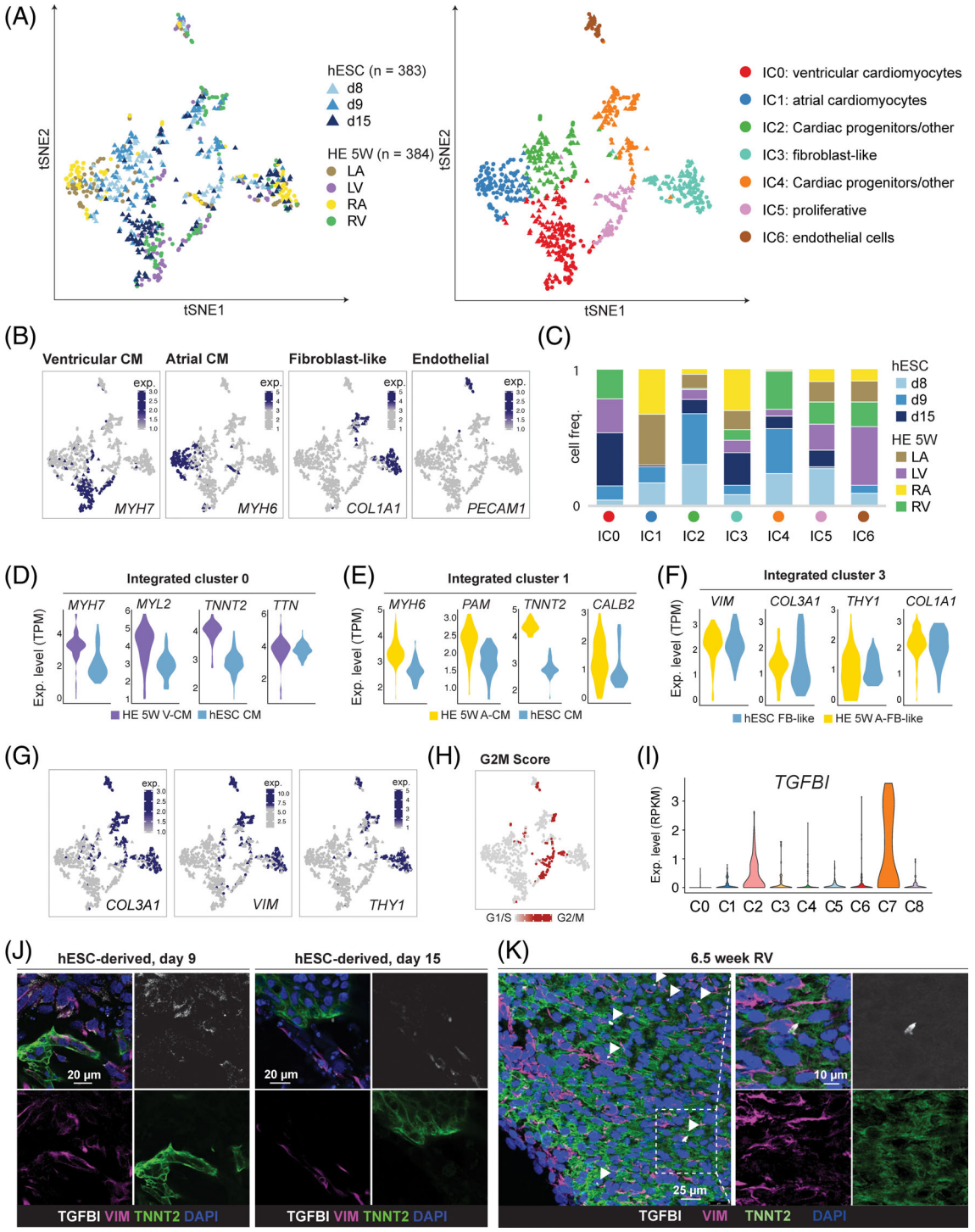

FIGURE 2 Single-cell comparison between hESC cardiac induction and human fetal heart development. A, T-SNE clustering of in vitro and in vivo cells.[1] Colors indicate cell origin, that is, time point for in vitro cells and spatial annotations (LA, left atrium; LV, left ventricle; RA, right atrium; RV, right ventricle) for in vivo cells. B, T-SNE feature plots indicating the expression of example marker genes for different cell types. C, Fractions of cells from different origins, that is, in vitro time points and in vivo spatial annotations in each cluster. D, Violin plots indicating ventricular marker gene expression by in vitro and in vivo cells in integrated cluster 0. E, Atrial marker gene expression by in vitro and in vivo cells in integrated cluster 1. F, Fibroblast marker gene expression by in vitro and in vivo cells in integrated cluster 3. G, Feature plots indicating the expression of fibroblast marker genes. H, Cell-cycle scores illustrated as a feature plot showing proliferating cells in red. I, Violin plot indicating specific expression of *TGFBI* by cluster 7 fibroblast-like cells in the complete in vitro dataset. J, in vitro fibroblast-like cells express TGFBI and cardiac fibroblast marker vimentin (VIM). K, in vivo fetal cardiac fibroblasts express both TGFBI and VIM

fibroblast-like cells (IC3), proliferative cardiac progenitors (IC5), and endothelial cells (IC6) (Figure 2A,B). IC2 and IC4 consist of early cardiac progenitors and small populations of other cell types. The hESC-derived endoderm population did not overlap with human fetal cells, but is included in IC4 as a separate population marked by *HNF4A* expression (supplemental online Figure 2D).

IC0 comprises of cells from 5W left and right ventricles and day 15 hESC-derived cardiomyocytes (Figure 2C). IC0 population expresses ventricle-specific genes such as *MYH7* (Figure 2D). IC1 cells express atrial-specific genes such as *MYH6* (Figure 2E) and the cluster comprises in vivo atrial cells and day-8 and -9 in vitro cells (Figure 2C). Remarkably, little to no day-15 cells were found in the atrial IC1 (Figure 2A,C). The in vitro cells of IC0 and IC1 correspond to the cardiomyocyte cluster of the in vitro dataset (C5). This in vivo transcriptomic comparison confirms that (a) the Wnt modulation-based differentiation protocol generates ventricular cardiomyocytes, in line with previous report,[11] and (b) human ventricular progenitors initially go through an atrial-like transcription program before differentiating into ventricular cardiomyocytes, in line with mouse studies.[28] Interestingly, in vivo ventricular and atrial cells expressed their respective lineage markers at a higher level compared with their in vitro counterparts (Figure 2D,E).

IC2 corresponds to the differentiating cardiomyocytes in vitro and clusters close to both the atrial (IC1) and ventricular cardiomyocytes (IC0) (Figure 2A). IC3 consists of cardiac fibroblast-like cells from both in vivo and in vitro (Figure 2B,C), expressing fibroblast and epicardial markers (Figure 2F,G, supplemental online Figure 2E). The in vitro cells in IC3 correspond to the C7 fibroblast-like cells (Figure 1C). IC4 corresponds to the early cardiac progenitors in vitro (C2). IC5 is a group of proliferative cardiac progenitors, based on the expression of G2M cell-cycle markers (Figure 2H), and expresses highly similar markers compared with IC0 and IC1. IC6 is a group of endothelial cells expressing *PECAM1* (Figure 2B).

We found that *TGFBI*, a TGF-β-responsive extracellular matrix gene, strongly marks the hESC-derived cardiac fibroblast-like cells (C7) (Figure 2I), which we verified by immunostaining TGFBI with fibroblast marker vimentin (VIM) and cardiomyocyte marker TNNT2 (Figure 2J). TGF-β signaling pathway plays an important role in the induction of epithelial-mesenchymal transition during cardiac development.[29] We found from an additional human fetal single-cell dataset,[30] that *TGFBI* is expressed in fibroblast-like and epicardium-derived cells in the 6.5 to 7W human fetal heart. We performed TGFBI immunostaining on human 6.5W and 10W fetal tissue together with VIM and TNNT2 (Figure 2K, supplemental online Figure 3A,B). In line with the sequencing results, we detected TGFBI and VIM coexpression at both fetal time points in cardiac ventricles, with expression more abundant in the RV (supplemental online Figure 3A). Interestingly, in 6.5W RV, *TGFBI* expressing cells were located close to epicardium (supplemental online Figure 3A). Taken together, our results indicate that TGFBI may be a specific marker of a subset of human embryonic cardiac fibroblasts both in vivo and in vitro.

In summary, we integrated in vivo and in vitro single-cell transcriptomic data to directly compare the two on a transcriptome-wide level. These analyses verified the cellular identity of in vitro-generated cells, and further validate the relevance of the hESC-based system to study early cardiac progenitors that cannot be obtained in vivo.

3.3 | Trajectory mapping reveals branch points in cardiac differentiation

In order to resolve the lineage relationship between the identified cell types, we sought to visualize the canonical cardiomyocyte differentiation axis and other noncanonical cell types. We used two methods: (a) a modified pipeline for graphical analysis by FDG[20] based on t-SNE dimensionality reduction (Figure 3A), and (b) Uniform Manifold Approximation and Projection (UMAP) (Figure 3B).[21,23] The original clustering was preserved on both FDG and UMAP (Figure 3A,B). Assessment of differences between batches indicates that batch effect is not the major driver of cellular heterogeneity (supplemental online Figure 4A).

The resulting FDG and UMAP revealed a continuous pluripotent to cardiomyocyte differentiation trajectory, as well as nonmyogenic lineages connected to the pluripotent cluster through bridges (Figure 3A,B). We confirmed the resulting trajectories are in line with pseudotime values calculated from Monocle (supplemental online Figure 4B). Both FDG and UMAP analyses indicate that multiple trajectories branch from pluripotent C0 cells (Figure 3A,B): (a) cardiac mesoderm (C1); (b) endoderm-like (C8); and (c) fibroblast-like (C7) (Figure 3A-C and supplemental online 4C). The fibroblast-like population (C7) is marked by *TGFBI* and *TFAP2A*, a transcription factor broadly expressed by ectodermal lineages as well as human cardiac fibroblasts[31] (Figure 3C). Interestingly, a subpopulation of C7 also expressed *SEMA3D*, a proepicardial progenitor and neural crest marker (supplemental online Figure 4C).[32] Cells at the beginning of the *HHEX*$^+$ endoderm trajectory expressed the early endoderm marker *SOX17*, whereas cells located closer to the tip of the trajectory express markers of endoderm derivatives such as *APOA2*[33] (Figure 3C and supplemental online Figure 4C).

The C1 cardiac mesoderm consists of proliferative and nonproliferative cells (Figure 3D). Interestingly, the nonproliferative C1 cells showed higher *ISL1* expression (Figure 3C). The C1 cardiac mesoderm is connected to the C2 early cardiac progenitors, which represent the well-studied ISL1 human cardiac progenitor.[30,34] Our trajectory mapping reconstructed a branching point at the C2 ISL1$^+$ early cardiac progenitors. Distinct trajectories emerge from the ISL1$^+$ population: a small group of endothelial cells marked by *PECAM1*expression (Figure 3C); a proliferative population of cells showing similar transcriptional profile as the C2 population (C3); and a trajectory of late cardiac progenitors and cardiomyocytes (C4 and C5) (Figure 3C, supplemental online Figure 4C). In addition, a population of smooth muscle-like cells marked by *ACTA2* expression was found embedded in the cardiomyocyte cluster (Figure 3C). Within the C2 ISL1$^+$ early cardiac progenitor, where the above populations stem from, we found a significant enrichment of extracellular matrix genes, such as *COL3A1*. *COL3A1* was also coexpressed with myogenic lineage markers *PDGFRA* and *NKX2-5* (Figure 3C,E). To validate the

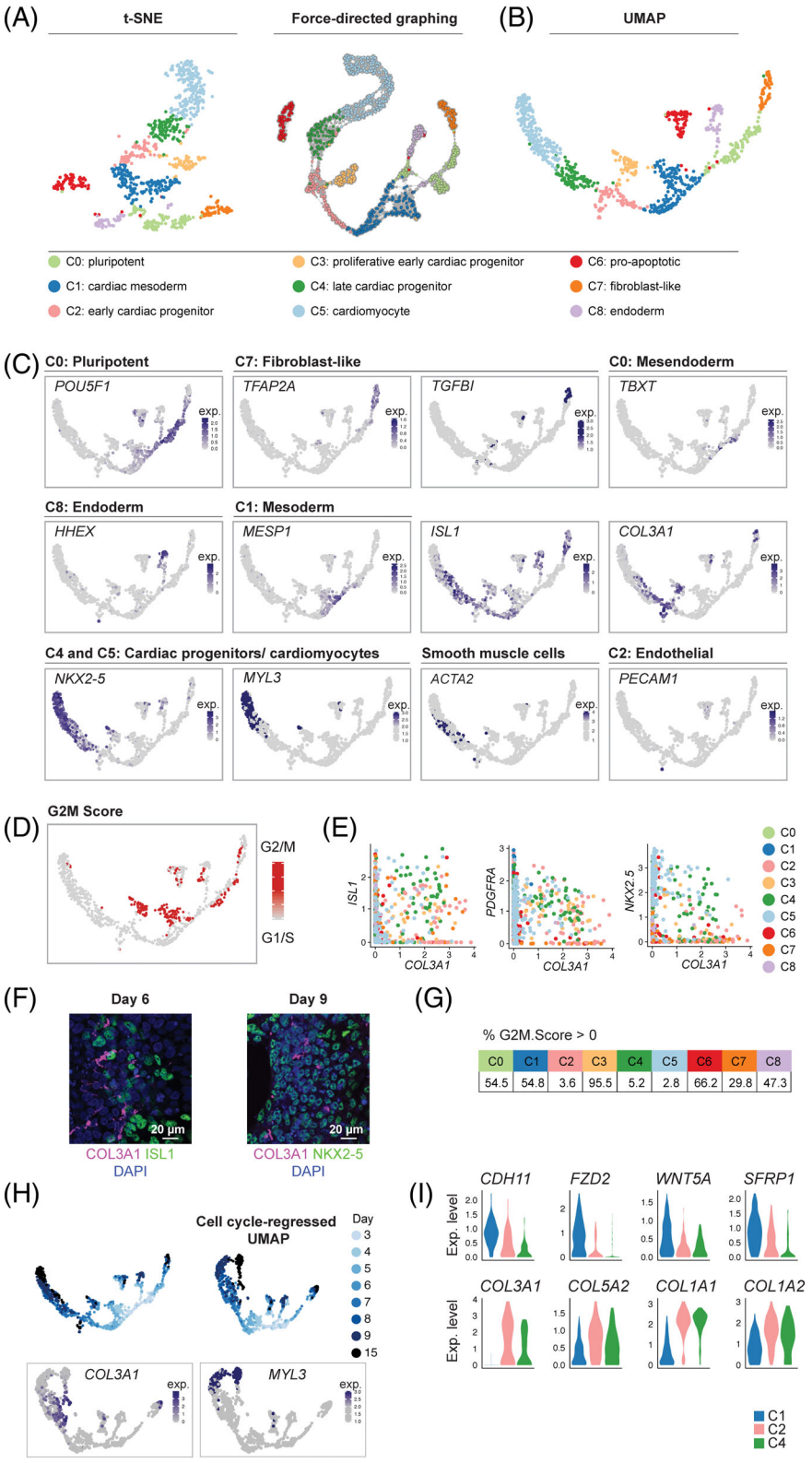

FIGURE 3 Trajectory analysis draws a detailed lineage map of hESC cardiac differentiation. A, T-SNE, FDG, and B, UMAP representation of single-cell transcriptomes. C, Example marker gene expression. Markers for pluripotency (*POU5F1*), fibroblast-like population (*TFAP2A* and *TGFBI*), mesendoderm (*TBXT*), endoderm (*HHEX*), mesoderm (*MESP1*), cardiac progenitors (*ISL1* and *COL3A1*), late cardiac progenitors (*NKX2-5*), cardiomyocytes (*MYL3*), smooth muscle-like cells (*ACTA2*) and endothelial cells (*PECAM1*). D, Feature plot indicating cells with positive cell-cycle scores for G2 and M phase. E, Scatter plots indicating that *COL3A1* is coexpressed with *ISL1*, *PDGFRA*, and *NKX2-5* in cardiac progenitors. F, Immunostaining indicating coexpression of COL3A1 with ISL1 and NKX2-5 in the cardiac progenitors. G, Percentages of cells with G2M scores >0 in each cluster. H, Original and cell-cycle regressed UMAP. Colors represent day and marker gene expression. I, Violin plot showing the expression of cadherin (*CDH11*), Wnt-related (*FZD2*, *WNT5A*, and *SFRP1*) and integrin signaling-related (*COL3A1*, *COL5A2*, *COL1A1*, and *COL1A2*) genes in clusters 1, 2, and 4

protein expression, we performed immunostaining of COL3A1, ISL1, and NKX2-5, which indicated that ISL1 progenitors expressed COL3A1 (Figure 3F).

We found that different cell populations were captured in various proliferative states. Therefore, we wanted to normalize the cell-cycle heterogeneity in order to account for the true transcriptomic differences between cell populations. We assigned each cell a cell-cycle score (G2M score), based on their expression of markers of G2 and M phase of the cell cycle (see the Methods section) (Figure 3D,G).

We observed that the C3 early cardiac progenitor population was the most proliferative population in our dataset. Since C2 and C3 are otherwise highly similar in their transcriptional identity, we hypothesized that this cell-cycle heterogeneity skewed the appearance of the myogenic lineage trajectory, and to mitigate the effect, we regressed out the cell-cycle phase scores and repeated clustering (see the Methods section). The resulting UMAP is highly similar except the C2 and C3 early cardiac progenitors are now fused together (Figure 3H). Together C2 and C3 likely represent the well-studied ISL1$^+$ human cardiac progenitor,[30,34] and the cell-cycle regressed trajectory suggests C2 and C3 collectively contribute to the cardiomyocyte differentiation trajectory (Figure 3H).

Next, we aimed to identify signaling pathways regulating lineage progression of the myogenic axis (C1, C2, and C4 specifically). Top 100 statistically significant marker genes of C1 and C2 were used as input for Panther pathway analysis tool.[35,36] We visualized the results within the three populations: cardiac mesoderm (C1), early cardiac progenitor (C2), and late cardiac progenitor (C4) (Figure 3I, supplemental online Table 6). Within C1, pathway analysis indicated significant enrichment of cadherin, angiogenesis, and Wnt signaling pathways. C1 showed specific expression of cadherin-11 (CDH11) (Figure 3I), a cell-cell adhesion molecule marking endothelial and endocardial cells, as well as mesenchymal smooth muscle cell progenitors.[37] In contrast to C1, C2, and C4 showed enrichment of integrin signaling-related genes, such as specific collagens (Figure 3I), suggesting that specific extracellular matrix-related genes play a role in myogenesis. Taken together, the cardiac mesoderm population has a highly active Wnt signaling pathway, whereas the specification of cardiac mesoderm into committed cardiac progenitors is characterized by increased integrin signaling.

In summary, the high temporal resolution of the data allowed the reconstruction of a continuous trajectory map of cardiac differentiation. Lineage trajectories could be defined, and the ISL1$^+$ human cardiac progenitor was found to be at a branching point between endothelial, cardiomyocyte, and smooth muscle lineages, in line with previous reports.[34] Furthermore, we observed that the ISL1$^+$ progenitors coexpressed specific extracellular matrix genes, which may play a role during development.

3.4 | RNA velocity confirms the existence of lineage branch points based on the detection of pre-mRNA

Trajectory analysis does not fully uncover the developmental dynamics of the differentiation process. RNA velocity, the time derivative of gene expression, can be used to predict the future state of individual cells by distinguishing between spliced and unspliced mRNAs.[17,38] Importantly, RNA velocity would also add directionality to the lineage trajectories. Based on this concept, using the detection of pre-mRNA sequences inherent in the dataset, we sought to generate lineage predictions, in order to study the transcriptional dynamics and to verify lineage trajectories.

We compared several methods to produce RNA velocity estimates provided by Le Manno et al, and found very similar results (see the Methods section) (supplemental online Figure 5). We visualized the RNA velocity calculations as a vector field showing regional average RNA velocities on the t-SNE, FDG, and UMAP plots, the length indicating the speed of the differentiation events (Figure 4A-C).

As expected, RNA velocity vectors of the C0 pluripotent population points toward the C1 mesoderm cells. The C7 fibroblast-like lineage has RNA velocity vectors pointing away from C0 and the other lineages, indicating that it is independent from the myogenic and endoderm trajectories.

Interestingly, RNA velocity vectors within the C1 cardiac mesoderm pointed backward in pseudotime, suggesting they might be maintaining an undifferentiated progenitor phenotype.

The C2 early cardiac progenitors have a relatively stable cellular state as indicated by short RNA velocity vectors, in contrast to the cardiomyocytes and endothelial cells, which have RNA velocity vectors pointing away from the C2 progenitors. The late cardiac progenitors and cardiomyocytes (C4 and C5) have RNA velocity vectors pointing toward the tip of the myogenic trajectory, suggesting strong cardiomyocyte lineage commitment.

Taken together, RNA velocity based on the detection of pre-mRNA provides the directionality of the lineage trajectories, which could only be inferred in previous analyses.

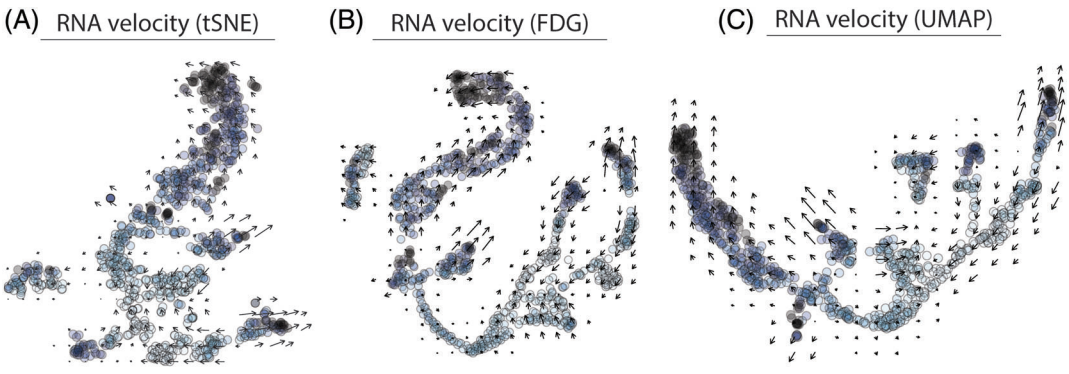

FIGURE 4 RNA velocity illustrates progenitor dynamics and clarifies trajectory branching points. A-C, RNA velocity based on t-SNE, FDG, and UMAP. Arrows indicate local average velocity on a regular grid vector field. Color represents time points

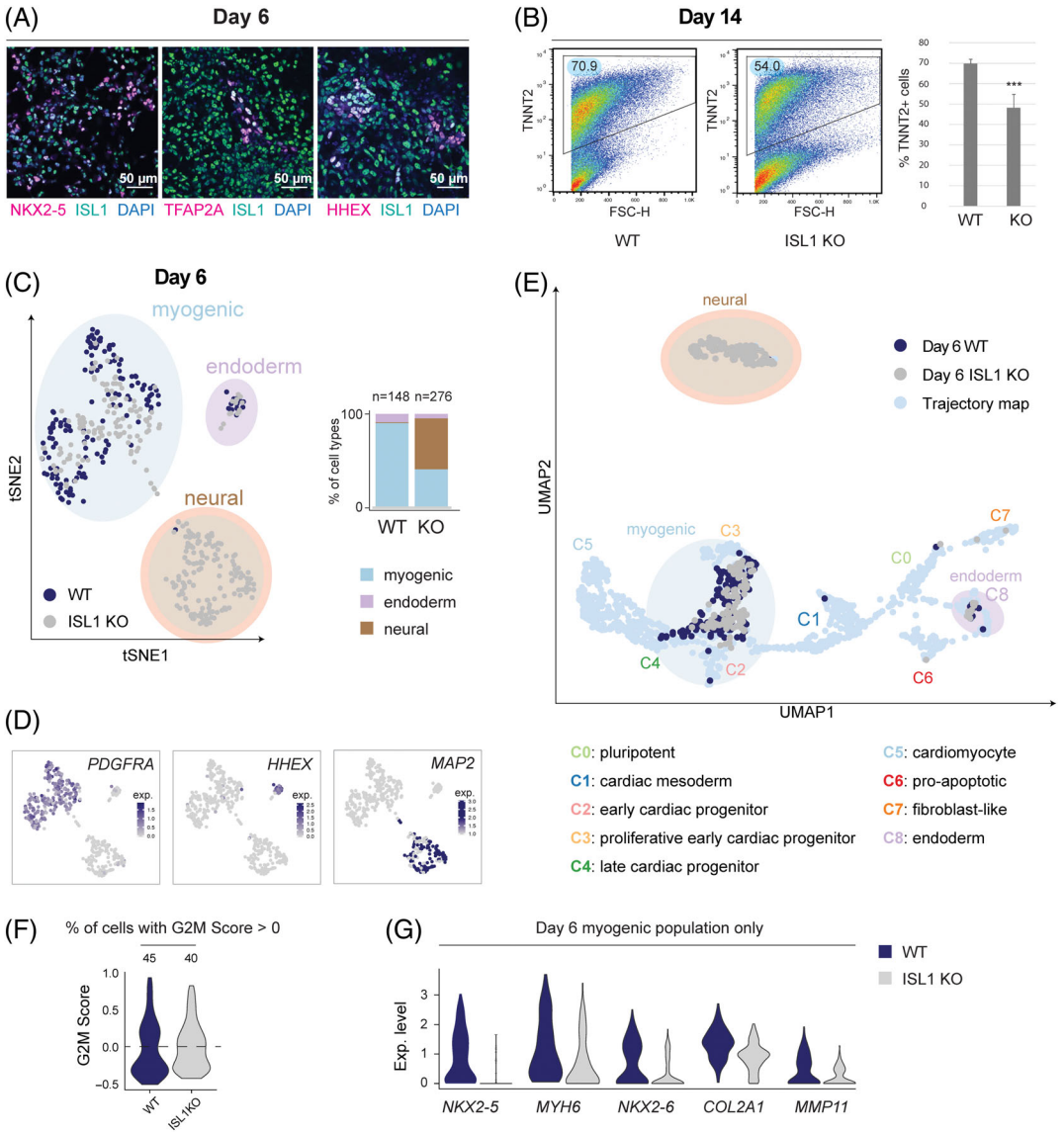

FIGURE 5 ISL1 is not required for the generation or proliferation of myogenic progenitors, but loss of ISL1 partially redirects myogenic progenitors toward a neural-like lineage. A, Immunostaining of ISL1 with lineage markers NKX2-5, TFAP2A, and HHEX at day 6 of hESC cardiac differentiation. B, Flow cytometry analysis and quantification showing TNNT2 expression at day 14 of cardiac differentiation by WT (n = 8) and KO (n = 8) cells. Error bars represent standard deviation. C, T-SNE clustering of combined day 6 WT and KO cells. Bar chart shows percentages of myogenic, neural, and endoderm populations per genotype. D, T-SNE feature plots indicating the expression of myogenic (*PDGFRA*), endoderm (*HHEX*), and neural (*MAP2*) marker genes in the day 6 WT and *ISL1* KO dataset. E, Day 6 WT and *ISL1* KO cells projected onto the UMAP of the full dataset. F, Violin plots indicating the cell-cycle scores of WT and *ISL1* KO cells within the myogenic population. G, Violin plots indicating differential expression between genes related to cardiac differentiation (*NKX2-5*, *MYH6*, and *NKX2-6*) and extracellular matrix organization (*COL2A1* and *MMP11*) in WT compared with *ISL1* KO cells within the myogenic population

3.5 | ISL1 marks and plays distinct roles in myogenic and nonmyogenic populations

Given that *ISL1* is expressed in the progenitors of both the myogenic and nonmyogenic trajectories (Figure 3C), we wanted to assess whether the different lineage progenitors are dependent on *ISL1* expression. We confirmed ISL1 protein expression using immunohistochemistry in the C4 myogenic (marked by NKX2.5) lineage, C8 endoderm-like (marked by HHEX) lineage, and the C7 fibroblast-like (marked by TFAP2A) lineage (Figure 5A).

An *ISL1* knockout (KO) hESC line was generated using the CRISPR/Cas9 system (supplemental online Figure 6A) and the loss of *ISL1* expression was verified (supplemental online Figure 6B). *ISL1* KO hESCs generated less TNNT2^{+} beating cardiomyocytes by day 14 compared to wild-type (WT) hESCs (Figure 5B). To assess the cell fate of WT vs *ISL1* KO progenitors, we proceeded with scRNA-seq of

the *ISL1* KO and WT cells at day 6. 276 *ISL1* KO and 148 WT cells passed quality control and were used for subsequent analyses.

The majority of day-6 WT cells were myogenic, marked by *PDGFRA*, with a small number of endoderm-like cells, marked by *HHEX* (Figure 5C,D, supplemental online Figure 6C). In contrast, the day-6 *ISL1* KO cells have a decreased proportion of myogenic progenitors (Figure 5C). Instead, the *ISL1* KO cells have an ectopic cell population expressing genes related to nervous system development, such as *MAP2*, *ZIC2*, *SOX2*, and *PAX3* (Figure 5C,D, supplemental online Figure 6C). We projected the *ISL1* KO cells onto the UMAP of the full dataset, and found that the neural-like population in the *ISL1* KO did not correspond to any other cell type in the UMAP (Figure 5E). The *ISL1* KO also produced a small number of endoderm-like cells, same as WT. Therefore, the *ISL1* KO studies suggest that ISL1 is not essential for the myogenic and endoderm lineages, but plays a role in suppressing a neural transcription program during myogenic differentiation.

Next, we wanted to determine whether *ISL1* expression is required for the proliferation of myogenic progenitors. Assessment of cell-cycle differences between the WT and *ISL1* KO myogenic progenitors indicated a similar percentage of proliferative cells in the *ISL1* KO myogenic lineage compared with the WT (Figure 5F), indicating that at the progenitor stage, loss of ISL1 does not affect proliferative capacity. Finally, we found that the expression of cardiogenic genes, such as *NKX2-5* and *MYH6*, and extracellular matrix organization-related genes, such as *COL2A1* and *MMP11*, was significantly decreased in the *ISL1* KO myogenic population compared to WT myogenic population (Figure 5G). We confirmed the decreased cardiogenic and extracellular matrix-related gene expression in days 6 and 10 by qPCR in several differentiation batches (supplemental online Figure 6D). In addition, qPCR analysis of endoderm markers indicated that the loss of ISL1 did not significantly affect endoderm differentiation in the in vitro differentiation.

Taken together, our results indicate that (a) ISL1 is not required for the generation of myogenic progenitors, but it plays an important role in suppressing a neural-like transcription program; (c) loss of ISL1 does not affect the proliferative capacity of myogenic progenitors; and (c) in the absence of ISL1 the expression of extracellular matrix-related and cardiogenic genes in myogenic progenitors are decreased.

4 | DISCUSSION

Cardiac induction of hESCs is routinely used for tissue engineering, regenerative medicine, and genetic perturbation studies. The cardiac induction protocol can also be manipulated to produce specific cellular subtypes, but this requires detailed knowledge of the signaling pathways involved in the lineage specification. Despite recent single-cell studies of the in vitro differentiation, the transient progenitors and lineage branch points have remained elusive.

This study captured day-by-day transcriptional changes covering the transition of pluripotent cells into cardiomyocytes and other cell types. High temporal resolution allowed us to connect the temporal snapshots into a continuous trajectory map, providing several important insights such as lineage branching points verified by pre-mRNA detection. Dimensional reduction techniques allowed us to generate a pseudotemporal ordering of cells, illustrating the differentiation and branching of pluripotent cells into mesoderm and endoderm, as well as $ISL1^+$ early cardiac progenitors into cardiomyocytes and endothelial cells. RNA velocity[17] was overlaid onto the trajectory map, confirming the pseudotemporal directionality. The population at the developmental juncture between cardiac mesoderm and committed cardiac progenitors is characterized by enrichment of integrin signaling-related genes, including expression of specific collagens. A previous study showed that day 6 of cardiac differentiation is the optimal time window for in vivo engraftment for hESC-derived cardiac progenitors,[11] which may partly be explained by the expression of extracellular matrix-related genes at this time point.

The in vitro-derived cardiac populations have previously been associated with fetal cardiac lineages based on marker genes and electrophysiological properties. Comparison between human in vivo and in vitro-generated cells in single-cell resolution provides an attractive method for the confirmation of population identities. We used this approach to verify the identity of hESC-derived cells using transcriptomic data from human embryonic heart.[1] During mammalian heart development, atrial genes (eg, *MYL4* and *MYL7*) are broadly expressed in both atria and ventricles, and later their expression becomes restricted to the atria.[28] In line with these findings, we found that cardiomyocytes collected on day 15 of cardiac differentiation matched transcriptionally best with human fetal ventricular cardiomyocytes, whereas the day-8 and day-9 progenitors, which later differentiated into ventricular cardiomyocytes, resembled fetal atrial cardiomyocytes. Earlier in vitro progenitors were developmentally more immature than the earliest cells that can feasibly be collected from human fetal hearts, highlighting the relevance of in vitro cardiac induction as a model system for the early human heart development.

Previous single-cell studies have reported definitive endoderm, outflow tract fibroblast, endothelial, mesenchymal, ectoderm, and neural crest populations in hESC cardiac induction.[12,13] The role of endoderm in cardiac lineage specification in in vivo heart development is well established,[39,40] and the presence of definitive endoderm population in the in vitro differentiation suggests that endoderm plays a role in the hESC cardiac induction. The previous studies have not comprehensively shown how the cardiac fibroblast-like cells relate to the cardiac differentiation trajectory.

Cardiac fibroblasts comprise a significant fraction of nonmyogenic cells in the mammalian heart[41] and are an attractive cell population for multiple purposes, such as tissue engineering. However, due to heterogeneity and lack of specific lineage markers, their function remains relatively unknown compared with other major cardiac cell types. We identified an in vitro-derived cardiac fibroblast-like population showing similar transcriptional profiles with human in vivo cardiac fibroblasts, and identified TGFBI as a candidate marker for these cells. Previous studies have indicated that the Wnt-modulation based cardiac induction protocol generates cardiac fibroblast-like cells,[13,42] but

their lineage has remained elusive. In the in vivo setting, majority of the cardiac fibroblasts arise from epicardium,[43-45] and some from endocardium[46,47] and neural crest.[46,48] Our lineage map suggests that the cardiac fibroblast-like population arise from a lineage trajectory that is separate from the myogenic lineage.

ISL1 has an important role regulating heart development[30,34,49] as well as in other organs,[50,51] and indeed, we found *ISL1* is expressed in both myogenic and nonmyogenic progenitors. Our genetic perturbation study indicated that ISL1 depletion partially redirects the myogenic cell fate toward nonmyogenic identities. Interestingly, *ISL1* deletion decreased the expression of extracellular matrix organization-related genes, which characterize the transition of cardiac mesoderm into cardiac progenitors. The robust enrichment of neural progenitors in *ISL1* KO differentiation suggests that ISL1 may play an inhibitory role of a neural program in cardiac progenitors, although ISL1 is required for motor neuron specification.[50]

5 | CONCLUSION

Our single-cell analysis uncovered developmental trajectories and lineage branching points of myogenic and nonmyogenic progenitors during hESC cardiac induction. The hESC cardiac differentiation is a useful model system for studying ISL1^{+} early cardiac progenitors, and our analysis further indicates ISL1 may be required to suppress a neural-like cell fate in myogenic progenitors.

ACKNOWLEDGMENTS

We thank Dr Makoto Sahara and Dr Peter Gruber for insightful suggestions and comments on the manuscript. We thank Dr Makoto Sahara for sharing the human cardiac sections for immunostaining. We thank Dr Jiejia Xu for sharing the *ISL1* knockout cell line. We thank Jesper Sohlmer and Kristine Bylund for providing assistance with Smart-Seq2 library preparation. We thank Dr Xidan Li, Dr Jianping Liu, Dr Byambajav Buyandelger and Sonja Gustafsson for providing assistance in sequencing and bioinformatics analysis. This work was supported by grants to K.R.C. from the Swedish Research Council (Research Collaboration Grant China-Sweden 539-2013-7002 and Distinguished Professor Grant 541-2013-8351), Wallenberg Foundation (KAW 2013.0028) and the European Research Council Advanced Research Grant Award (AdG743225) and C.Y.L. was partly funded by the Croucher Foundation through a Croucher fellowship.

CONFLICT OF INTEREST

K.R.C declared advisory role and research funding from EQT-AstraZeneca and stock ownership in SWIB-Procella-Smartwise-Moderna. The other authors declared no potential conflicts of interest.

AUTHOR CONTRIBUTIONS

M.M., C.Y.L.: conception and design, collection and assembly of data, data analysis and interpretation, manuscript writing; J.X.: provision of study material or patients, data analysis and interpretation; K.C.: conception and design, financial support, data analysis and interpretation, manuscript writing, final approval of manuscript.

DATA AVAILABILITY STATEMENT

The data that support the findings of this study are available on request from the corresponding author.

ORCID

Mimmi M. Mononen https://orcid.org/0000-0002-6096-8887

REFERENCES

1. Jia G, Preussner J, Chen X, et al. Single cell RNA-seq and ATAC-seq analysis of cardiac progenitor cell transition states and lineage settlement. *Nat Commun*. 2018;9:4877.
2. Lescroart F, Wang X, Lin X, et al. Defining the earliest step of cardiovascular lineage segregation by single-cell RNA-seq. *Science*. 2018; 359:1177-1181.
3. Chan SS, Chan HHW, Kyba M. Heterogeneity of Mesp1+ mesoderm revealed by single-cell RNA-seq. *Biochem Biophys Res Commun*. 2016; 474:469-475.
4. DeLaughter DM, Bick AG, Wakimoto H, et al. Single-cell resolution of temporal gene expression during heart development. *Dev Cell*. 2016; 39:480-490.
5. Scialdone A, Tanaka Y, Jawaid W, et al. Resolving early mesoderm diversification through single-cell expression profiling. *Nature*. 2016; 535:289-293.
6. Cui Y, Zheng Y, Liu X, et al. Single-cell transcriptome analysis maps the developmental track of the human heart. *Cell Rep*. 2019;26:1934-1950. e1935.
7. Sahara M, Santoro F, Sohlmer J, et al. Population and single-cell analysis of human cardiogenesis reveals unique LGR5 ventricular progenitors in embryonic outflow tract. *Dev Cell*. 2019;48:475-490. e477.
8. Burridge PW, Matsa E, Shukla P, et al. Chemically defined generation of human cardiomyocytes. *Nat Methods*. 2014;11:855-860.
9. Lian X, Hsiao C, Wilson G, et al. Robust cardiomyocyte differentiation from human pluripotent stem cells via temporal modulation of canonical Wnt signaling. *Proc Natl Acad Sci U S A*. 2012;109:E1848-E1857.
10. Lian X, Zhang J, Azarin SM, et al. Directed cardiomyocyte differentiation from human pluripotent stem cells by modulating Wnt/beta-catenin signaling under fully defined conditions. *Nat Protoc*. 2013;8:162-175.
11. Foo KS, Lehtinen ML, Leung CY, et al. Human ISL1(+) ventricular progenitors self-assemble into an in vivo functional heart patch and preserve cardiac function post infarction. *Mol Ther*. 2018;26:1644-1659.
12. Churko JM, Garg P, Treutlein B, et al. Defining human cardiac transcription factor hierarchies using integrated single-cell heterogeneity analysis. *Nat Commun*. 2018;9:4906.
13. Friedman CE, Nguyen Q, Lukowski SW, et al. Single-cell transcriptomic analysis of cardiac differentiation from human PSCs reveals HOPX-dependent cardiomyocyte maturation. *Cell Stem Cell*. 2018;23: 586-598. e588.
14. Liu Z, Wang L, Welch JD, et al. Single-cell transcriptomics reconstructs fate conversion from fibroblast to cardiomyocyte. *Nature*. 2017;551:100-104.
15. Poon E, Yan B, Zhang S, et al. Transcriptome-guided functional analyses reveal novel biological properties and regulatory hierarchy of human embryonic stem cell-derived ventricular cardiomyocytes crucial for maturation. *PLoS One*. 2013;8:e77784.
16. Ruan H, Liao Y, Ren Z, et al. Single-cell reconstruction of differentiation trajectory reveals a critical role of ETS1 in human cardiac lineage commitment. *BMC Biol*. 2019;17:89.

17. La Manno G, Soldatov R, Zeisel A, et al. RNA velocity of single cells. *Nature*. 2018;560:494-498.
18. Picelli S, Bjorklund AK, Faridani OR, Sagasser S, Winberg G, Sandberg R. Smart-seq2 for sensitive full-length transcriptome profiling in single cells. *Nat Methods*. 2013;10:1096-1098.
19. Picelli S, Faridani OR, Bjorklund AK, Winberg G, Sagasser S, Sandberg R. Full-length RNA-seq from single cells using Smart-seq2. *Nat Protoc*. 2014;9:171-181.
20. Kee N, Volakakis N, Kirkeby A, et al. Single-cell analysis reveals a close relationship between differentiating dopamine and subthalamic nucleus neuronal lineages. *Cell Stem Cell*. 2017;20:29-40.
21. Butler A, Hoffman P, Smibert P, Papalexi E, Satija R. Integrating single-cell transcriptomic data across different conditions, technologies, and species. *Nat Biotechnol*. 2018;36:411-420.
22. Satija R, Farrell JA, Gennert D, Schier AF, Regev A. Spatial reconstruction of single-cell gene expression data. *Nat Biotechnol*. 2015;33:495-502.
23. Stuart T, Butler A, Hoffman P, et al. Comprehensive integration of single-cell data. *Cell*. 2019;177:1888-1902. e1821.
24. Szklarczyk D, Gable AL, Lyon D, et al. STRING v11: protein-protein association networks with increased coverage, supporting functional discovery in genome-wide experimental datasets. *Nucleic Acids Res*. 2019;47:D607-D613.
25. Trapnell C, Cacchiarelli D, Grimsby J, et al. The dynamics and regulators of cell fate decisions are revealed by pseudotemporal ordering of single cells. *Nat Biotechnol*. 2014;32:381-386.
26. Qiu X, Hill A, Packer J, Lin D, Ma YA, Trapnell C. Single-cell mRNA quantification and differential analysis with census. *Nat Methods*. 2017;14:309-315.
27. Qiu X, Mao Q, Tang Y, et al. Reversed graph embedding resolves complex single-cell trajectories. *Nat Methods*. 2017;14:979-982.
28. Zammit PS, Kelly RG, Franco D, Brown N, Moorman AF, Buckingham ME. Suppression of atrial myosin gene expression occurs independently in the left and right ventricles of the developing mouse heart. *Dev Dyn*. 2000;217:75-85.
29. von Gise A, Pu WT. Endocardial and epicardial epithelial to mesenchymal transitions in heart development and disease. *Circ Res*. 2012;110:1628-1645.
30. Cai CL, Liang X, Shi Y, et al. Isl1 identifies a cardiac progenitor population that proliferates prior to differentiation and contributes a majority of cells to the heart. *Dev Cell*. 2003;5:877-889.
31. Ross GR, Edwards S, Warner C, et al. Deletion of transcription factor AP-2alpha gene attenuates fibroblast differentiation into myofibroblast. *J Cell Mol Med*. 2019;23:6494-6498.
32. Katz TC, Singh MK, Degenhardt K, et al. Distinct compartments of the proepicardial organ give rise to coronary vascular endothelial cells. *Dev Cell*. 2012;22:639-650.
33. Wang P, Rodriguez RT, Wang J, Ghodasara A, Kim SK. Targeting SOX17 in human embryonic stem cells creates unique strategies for isolating and analyzing developing endoderm. *Cell Stem Cell*. 2011;8:335-346.
34. Bu L, Jiang X, Martin-Puig S, et al. Human ISL1 heart progenitors generate diverse multipotent cardiovascular cell lineages. *Nature*. 2009;460:113-117.
35. Mi H, Muruganujan A, Ebert D, Huang X, Thomas PD. PANTHER version 14: more genomes, a new PANTHER GO-slim and improvements in enrichment analysis tools. *Nucleic Acids Res*. 2019;47:D419-D426.
36. Mi H, Thomas P. PANTHER pathway: an ontology-based pathway database coupled with data analysis tools. *Methods Mol Biol*. 2009;563:123-140.
37. Alimperti S, Andreadis ST. CDH2 and CDH11 act as regulators of stem cell fate decisions. *Stem Cell Res*. 2015;14:270-282.
38. Svensson V, Pachter L. RNA velocity: molecular kinetics from single-cell RNA-Seq. *Mol Cell*. 2018;72:7-9.
39. Nascone N, Mercola M. An inductive role for the endoderm in Xenopus cardiogenesis. *Development*. 1995;121:515-523.
40. Schultheiss TM, Xydas S, Lassar AB. Induction of avian cardiac myogenesis by anterior endoderm. *Development*. 1995;121:4203-4214.
41. Pinto AR, Ilinykh A, Ivey MJ, et al. Revisiting cardiac cellular composition. *Circ Res*. 2016;118:400-409.
42. Zhang J, Tao R, Campbell KF, et al. Functional cardiac fibroblasts derived from human pluripotent stem cells via second heart field progenitors. *Nat Commun*. 2019;10:2238.
43. Witty AD, Mihic A, Tam RY, et al. Generation of the epicardial lineage from human pluripotent stem cells. *Nat Biotechnol*. 2014;32:1026-1035.
44. Iyer D, Gambardella L, Bernard WG, et al. Robust derivation of epicardium and its differentiated smooth muscle cell progeny from human pluripotent stem cells. *Development*. 2015;142:1528-1541.
45. Guadix JA, Orlova VV, Giacomelli E, et al. Human pluripotent stem cell differentiation into functional epicardial progenitor cells. *Stem Cell Reports*. 2017;9:1754-1764.
46. Moore-Morris T, Guimaraes-Camboa N, Banerjee I, et al. Resident fibroblast lineages mediate pressure overload-induced cardiac fibrosis. *J Clin Invest*. 2014;124:2921-2934.
47. Wessels A, van den Hoff MJ, Adamo RF, et al. Epicardially derived fibroblasts preferentially contribute to the parietal leaflets of the atrioventricular valves in the murine heart. *Dev Biol*. 2012;366:111-124.
48. Ali SR, Ranjbarvaziri S, Talkhabi M, et al. Developmental heterogeneity of cardiac fibroblasts does not predict pathological proliferation and activation. *Circ Res*. 2014;115:625-635.
49. Moretti A, Caron L, Nakano A, et al. Multipotent embryonic isl1+ progenitor cells lead to cardiac, smooth muscle, and endothelial cell diversification. *Cell*. 2006;127:1151-1165.
50. Pfaff SL, Mendelsohn M, Stewart CL, Edlund T, Jessell TM. Requirement for LIM homeobox gene Isl1 in motor neuron generation reveals a motor neuron-dependent step in interneuron differentiation. *Cell*. 1996;84:309-320.
51. Zhuang S, Zhang Q, Zhuang T, Evans SM, Liang X, Sun Y. Expression of Isl1 during mouse development. *Gene Expr Patterns*. 2013;13:407-412.

SUPPORTING INFORMATION

Additional supporting information may be found online in the Supporting Information section at the end of this article.

How to cite this article: Mononen MM, Leung CY, Xu J, Chien KR. Trajectory mapping of human embryonic stem cell cardiogenesis reveals lineage branch points and an ISL1 progenitor-derived cardiac fibroblast lineage. *Stem Cells*. 2020;38:1267–1278. https://doi.org/10.1002/stem.3236